JOURNAL OF COMPUTATIONAL PHYSICS 87, 108–125 (1990)

Pseudo-spectral Solution of Nonlinear Schrödinger Equations

D. PATHRIA

Department of Computer Science, University of Waterloo, Waterloo, Canada N2L 3G1

AND

J. LL. MORRIS

Department of Mathematics and Computer Science, University of Dundee, Dundee DD1 4HN, Scotland

Received November 14, 1988; revised March 28, 1989

We compare four pseudo-spectral split-step methods for solving a class of nonlinear Schrödinger (NLS) equations. The importance of observing the L^2 invariance of the continuous problem is demonstrated through numerical experiments. The best performance is obtained by transforming the given equation to an NLS equation where two of the coefficients satisfy a simple algebraic relationship. The problem can be solved efficiently in terms of the new variables, and the l^2 norm of the computed solution is time-invariant.

1. INTRODUCTION

A generalized nonlinear Schrödinger equation (GNLS)

$$iu_t + u_{xx} + q_c |u|^2 u + q_q |u|^4 u + iq_m |u|^2{}_x u + iq_u |u|^2 u_x = 0 \tag{1.1}$$

governs the modulation of a quasi-monochromatic wave train in a weakly nonlinear, dispersive medium. We are considering the initial value problem with $u(x, 0) = u_0(x)$ specified, and where $i^2 = -1$, and q_c, q_q, q_m, and q_u are real parameters. Equation (1.1) was derived independently by Johnson [1] and Kakutani and Michihiro [2] to describe the behaviour of the Stokes wave near the state of modulational instability. (Although Johnson's equation contains a term in $u\zeta_t$, where $\zeta_x = |u|^2$, this may be eliminated as shown in [2].) The GNLS also has wide applicability as a model equation for a large class of evolutionary systems where the relevant time and space scales are greater than those captured by the

0021-9991/90 $3.00

usual nonlinear Schrödinger equation with a cubic nonlinearity [3]. It contains, as special cases,

$$iu_t + u_{xx} + q_c |u|^2 u = 0 \tag{1.2}$$

$$iu_t + u_{xx} + iq_m(|u|^2 u)_x = 0 \tag{1.3}$$

$$iu_t + u_{xx} + iq_u |u|^2 u_x = 0 \tag{1.4}$$

$$iu_t + u_{xx} + q_c |u|^2 u + q_q |u|^4 u = 0. \tag{1.5}$$

Equation (1.2) is the well-known cubic Schrödinger equation, which has important applications in fluid dynamics [4], nonlinear optics [5], and plasma physics [6]. The derivative nonlinear Schrödinger equation (1.3) governs the propagation of circular polarized nonlinear Alfvén waves in plasmas [7]. Equation (1.4) describes the self-modulation of the complex amplitude of solutions of the Benjamin–Ono equation [8], and the cubic–quintic Schrödinger equation (1.5) the propagation of laser beams in an inhomogeneous medium [9]. Equations (1.2)–(1.4) are particularly interesting, being completely integrable [10, 11], and admit, for certain initial conditions, soliton solutions.

As a further consequence of their complete integrability, those solutions of (1.2)–(1.4) which decay rapidly as $x \to \pm\infty$ satisfy an infinite number of conservation laws. For the general equation (1.1), rapidly decaying solutions (or periodic solutions, in which case integration is performed over one space period) are known to satisfy three conservation laws [12]

$$\int_{-\infty}^{\infty} |u|^2 \, dx = e_0 \tag{1.6}$$

$$\int_{-\infty}^{\infty} \left(|u_x|^2 - \frac{1}{2}(2q_m + q_u) |u|^2 \operatorname{Im}(u\bar{u}_x) - \frac{1}{2} q_c |u|^4 + \frac{1}{6}[q_m(2q_m + q_u) - 2q_q] |u|^6 \right) dx = e_1 \tag{1.7}$$

$$\int_{-\infty}^{\infty} [2 \operatorname{Im}(u\bar{u}_x) - q_m |u|^4] \, dx = e_2, \tag{1.8}$$

where the e_i are real constants, independent of time. The first of these, Eq. (1.6), represents the conservation of mass or L^2 norm of the system, and we refer to Eqs. (1.7) and (1.8) as the conservation of energy and impulse respectively.

In devising numerical schemes for the cubic Schrödinger equation, considerable attention has been paid to observing the discrete counterpart of (1.6) [13], and even of (1.7) [14], although the advantages gained by doing so are not clear [15, 16]. The conservation of the invariants is more difficult to enforce when the additional nonlinearities are included in the equation, and the need for doing so remains to be established.

We consider here four pseudo-spectral split-step methods for solving the initial value problem for (1.1). The first method conserves the mass in the discretized system, but requires the formation of expensive convolution sums. We then propose two alternative schemes, which considerably reduce the execution costs by sacrificing the invariance property. The convolution in the first method is unnecessary if $2q_m + q_u = 0$, and the transformation of an arbitrary GNLS to one satisfying this condition forms the basis of the fourth algorithm. We compare the methods through a number of numerical tests, and demonstrate the value of maintaining the mass invariance in the discrete system.

2. Pseudo-spectral Split-Step Methods

To solve the GNLS numerically we write it in the form

$$\partial_t u = \mathscr{S} u, \tag{2.1}$$

where $\mathscr{S}$ is the spatial differential operator acting on $u(x, t)$, defined by

$$\mathscr{S} = i\partial_x{}^2 + iq_c |u|^2 + iq_q |u|^4 - q_m |u|^2{}_x - q_u |u|^2 \partial_x. \tag{2.2}$$

With such a representation we can consider the spatial approximation independently of the time integration.

We solve for $u(x, t)$ on the finite rectangular grid $(x, t) \in [a, b] \times [0, T]$. Since the GNLS is invariant under a translation in space, we can, for convenience and without loss of generality, consider the interval centered about $x = 0$. The spatial domain is uniformly discretized at $n+1$ nodes x_j, $j = -n/2, ..., n/2$ with grid spacing $\Delta x = (b-a)/n$, and the solution is computed at times $t_m = m \times \Delta t$, Δt being the constant time step, for $0 < t_m \leqslant T$. We let $U(x, t)$ be the approximation to $u(x, t)$, and denote by subscripts and superscripts the approximations to $u(x, t)$ on the spatial and temporal grid points respectively. Hence, $U_j(t)$ denotes $U(x_j, t)$, and $U_j^m \approx u(x_j, t_m)$ is the approximation in the fully discretized system. U_j^0 is determined by the initial condition, $U_j^0 = u_0(x_j)$ for $j = -n/2, ..., n/2$.

We first consider the discretization of the space variable. If $u(x, t)$ is periodic on the spatial domain, and if $u(x, t)$ and $u_x(x, t)$ are piecewise continuous there, then $u(x, t)$ may be represented by the Fourier series

$$u(x, t) = \sum_{k=-\infty}^{\infty} \hat{u}_k(t) \exp i\mu_k x, \tag{2.3}$$

where

$$\mu_k = \frac{2\pi k}{b-a} \tag{2.4}$$

and where the Fourier coefficients are defined by

$$\hat{u}_k(t) = \frac{1}{b-a}\int_a^b u(x, t) \exp -i\mu_k x \, dx. \tag{2.5}$$

The computed approximation of (2.3) is a truncated Fourier series determined by the discrete function values at the n collocation nodes (the assumption of spatial periodicity reduces the number of degrees of freedom by one). On the grid points the interpolating polynomial has the form

$$\mathcal{F}_j^{-1}[\hat{U}] = U_j = \frac{1}{\sqrt{n}} \sum_{k=-n/2}^{n/2-1} \hat{U}_k \exp i\mu_k x_j, \tag{2.6}$$

with Fourier coefficients calculated according to

$$\mathcal{F}_k[U] = \hat{U}_k = \frac{1}{\sqrt{n}} \sum_{j=-n/2}^{n/2-1} U_j \exp -i\mu_j x_k. \tag{2.7}$$

Spatial derivatives are formed by analytically differentiating the interpolating polynomial and, letting D_x denote the approximation to ∂_x, at the grid points

$$\left.\frac{\partial^p u(x, t)}{\partial x^p}\right|_{x=x_j} \approx D_x{}^p U_j(t) = \frac{1}{\sqrt{n}} \sum_{j=-n/2}^{n/2-1} (i\mu_k)^p \, \hat{U}_k(t) \exp i\mu_k x_j. \tag{2.8}$$

Calculation of derivatives using function expansion techniques generally requires $O(n^2)$ operations. However, since the collocation nodes are uniformly spaced, the fast Fourier transform (FFT) may be used, at $O(n \log n)$ cost, to transform the problem to Fourier space, where derivatives can be inexpensively formed [17]. If n is a power of 2, the speed of the FFT is exploited to the fullest and so we limit our discussion to the case $n = 2^N$, with N an integer. For convenience, we drop the indices on the summation symbols and adopt the convention that $\sum$ denotes summation from $-n/2$ to $n/2-1$, unless otherwise indicated.

The semi-discrete system defined by the finite Fourier representation possesses analogues of the conservation laws (1.6)–(1.8), namely,

$$\frac{d}{dt}\sum_j |U_j|^2 = 0 \tag{2.9}$$

$$\frac{d}{dt}\sum_j \Big(|D_x U_j|^2 - \frac{1}{2}(2q_m + q_u)\,|U_j|^2 \operatorname{Im}(U_j D_x \bar{U}_j) - \frac{q_c}{2}|U_j|^4 + \frac{1}{6}(q_m(2q_m + q_u) - 2q_q)\,|U_j|^6 \Big) = 0 \tag{2.10}$$

$$\frac{d}{dt}\sum_j (2 \operatorname{Im}(U_j D_x \bar{U}_j) - q_m |U_j|^4) = 0. \tag{2.11}$$

It admits exactly the nonlinear dispersion relation of the differential equation, and the approximation enjoys spectral accuracy, that is, for sufficiently smooth functions, the interpolation error decays faster than any power of n [18].

We now consider the time integration procedure, suppressing for the moment the approximation in the spatial dimension. Formally, (2.1) has the solution

$$u(x, t_m + \Delta t) = \exp \int_{t_m}^{t_m + \Delta t} \mathscr{S}(\tau)\, d\tau \cdot u(x, t_m), \tag{2.12}$$

where for brevity we use $\mathscr{S}(\tau)$ to represent $\mathscr{S}(\tau, u(x, \tau))$. The integral in (2.12) can be approximated by a first-order right-hand rectangular rule,

$$\int_{t_m}^{t_m + \Delta t} \mathscr{S}(\tau)\, d\tau = \Delta t \mathscr{S}(t_m) + O(\Delta t^2), \tag{2.13}$$

and the exponential by decomposing $\mathscr{S}$ into three suboperators

$$\mathscr{S} = \mathscr{L} + \mathscr{M} + \mathscr{N}, \tag{2.14}$$

where

$$\mathscr{L} = i\, \partial_x^2 \tag{2.15}$$

$$\mathscr{M} = -q_m |u|^2{}_x - q_u |u|^2\, \partial_x \tag{2.16}$$

$$\mathscr{N} = iq_c |u|^2 + iq_q |u|^4. \tag{2.17}$$

The resulting exponential

$$u(x, t_m + \Delta t) \approx \exp \Delta t \mathscr{S}(t_m) \cdot u(x, t_m) = \exp \Delta t(\mathscr{L}(t_m) + \mathscr{M}(t_m) + \mathscr{N}(t_m)) \cdot u(x, t_m) \tag{2.18}$$

may then be approximated by the first-order splitting

$$u(x, t_m + \Delta t) = \exp \Delta t \mathscr{L}(t_m) \cdot \exp \Delta t \mathscr{M}(t_m) \cdot \exp \Delta t \mathscr{N}(t_m) \cdot u(x, t_m) + O(\Delta t^2), \tag{2.19}$$

which is exact in the special case that $\mathscr{L}$, $\mathscr{M}$, and $\mathscr{N}$ commute. Higher order splittings are possible [19] but we restrict our attention here to the first-order method (2.19).

If considered separately, the advancements in time for $\mathscr{N}$ and $\mathscr{L}$ are performed, in physical space and Fourier space respectively, according to

$$u(x, t_{m+1}) = \exp \Delta t \mathscr{N}(t_m) \cdot u(x, t_m) \colon U^{m+1} = \exp i(q_c |U^m|^2 + q_q |U^m|^4)\, \Delta t \cdot U^m \tag{2.20}$$

$$u(x, t_{m+1}) = \exp \Delta t \mathscr{L}(t_m) \cdot u(x, t_m) \colon U^{m+1} = \mathscr{F}^{-1}[\exp -i\mu_k{}^2\, \Delta t \cdot \mathscr{F}_k[U^m]], \tag{2.21}$$

and the mass invariance is maintained by both approximations.

Equations (2.20) and (2.21) are sufficient to form the split-step methods for the cubic Schrödinger equation [20–22] and the cubic–quintic Schrödinger equation [23]. The method is particularly well suited to these equations, since the derivative terms appear only linearly and the time stepping in Fourier space can be accomplished without the formation of convolution sums. Therefore, in the absence of the nonlinear derivative terms, $q_u = q_m = 0$, the method is readily obtained from (2.19) by sequentially applying the stages (2.20) and (2.21). The time integration is explicit in the nonlinear term, Eq. (2.20), but implicit in the linear, Eq. (2.21), and is therefore appropriate for the pseudo-spectral discretization. The $O(n \log n)$ cost of transforming between physical and Fourier space discourages the use of nonlinearly implicit time integration schemes, which must be solved by iteration.

Taha and Ablowitz note that the simple nonlinearity of the cubic Schrödinger equation may account for the success of the split-step method for that problem [22]. Indeed, the presence of the nonlinear derivative term in the GNLS complicates the observance of the l^2 invariance. While derivatives are accurately approximated in Fourier space, nonlinearities are more economically evaluated in physical space, their Fourier representation requiring the formation of convolution sums, at a cost corresponding to the strength of the nonlinearity. This cost can be avoided by integrating in physical space, but then the l^2 invariance of the computed solution is lost. The value of this invariance, in terms of the cubic Schrödinger equation, has been the subject of some debate. Herbst, Mitchell, and Weideman [24] encounter the nonphysical blowing up of solutions when the mass is not conserved. In other studies, however, the invariance property appears to be neither necessary nor sufficient for reasonable results [15, 16]. We therefore examine the need for mass invariance in the numerical solution of the GNLS, and present four methods which differ in their treatment of $\mathcal{M}$, and which consequently exhibit different conservation properties.

2.1. *Method PS1*

A simple rearrangement of the nonlinear derivative terms allows the GNLS to be written in an equivalent form,

$$iu_t + u_{xx} + q_c |u|^2 u + q_q |u|^4 u - 2q_m \operatorname{Im}(u\bar{u}_x) + i(2q_m + q_u) |u|^2 u_x = 0. \quad (2.1.1)$$

Hence $\mathcal{M}$ can be expressed as

$$\mathcal{M} = -2iq_m \operatorname{Im}(u\bar{u}_x) - (2q_m + q_u) |u|^2 \partial_x \quad (2.1.2)$$

and may be split further into the two operators

$$\mathcal{M}_1 = -2iq_m \operatorname{Im}(u\bar{u}_x) \quad (2.1.3)$$

$$\mathcal{M}_2 = -(2q_m + q_u) |u|^2 \partial_x. \quad (2.1.4)$$

The advancements according to each of these, considered separately, become

$$u(x, t_{m+1}) = \exp \Delta t \mathscr{M}_1 \cdot u(x, t_m)\colon U^{m+1} = \exp -2iq_m \operatorname{Im}(U_m \partial_x \bar{U}^m)\, \Delta t \cdot U^m \tag{2.1.5}$$

$$u(x, t_{m+1}) = \exp \Delta t \mathscr{M}_2 \cdot u(x, t_m)\colon U^{m+1} = \mathscr{F}^{-1}[\exp -i(2q_m + q_u)\mu_k B_k\, \Delta t \cdot \mathscr{F}_k[U^m]]. \tag{2.1.6}$$

Here B, the convolution sum due to representing $|u|^2$ term in Fourier space, satisfies

$$\sum_k i\mu_k B_k \hat{U}_k \exp i\mu_k x_j = \frac{1}{n} \sum_{k_1} \sum_{k_2} \sum_{k_3} i\mu_{k_3} \hat{U}_{k_1} \bar{\hat{U}}_{k_2} \hat{U}_{k_3} \exp i(\mu_{k_1} - \mu_{k_2} + \mu_{k_3}) x_j, \tag{2.1.7}$$

with $B_k := 0$ if $|\mu_k \hat{U}_k|$ is less than some specified tolerance.

When applied successively on the spatially discrete problem, the individual time stepping schemes yield the fully discrete algorithm PS1 for computing U_j^{m+1},

$$U_j^{(0)} = \exp i(q_c |U_j^m|^2 + q_q |U_j^m|^4)\, \Delta t \cdot U_j^m \tag{2.1.8}$$

$$U_j^{(1)} = \exp -2iq_m \operatorname{Im}(U_j^{(0)} D_x \bar{U}_j^{(0)})\, \Delta t \cdot U_j^{(0)} \tag{2.1.9}$$

$$U_j^{(2)} = \mathscr{F}_j^{-1}[\exp -i(2q_m + q_u) B_k \mu_k\, \Delta t \cdot \mathscr{F}_k[U_j^{(1)}]] \tag{2.1.10}$$

$$U_j^{m+1} = \mathscr{F}_j^{-1}[\exp -i\mu_k^2\, \Delta t \cdot \mathscr{F}_k[U_j^{(2)}]], \tag{2.1.11}$$

where B_k is defined by (2.1.7) and where $U_j^{(0)}$, $U_j^{(1)}$, and $U_j^{(2)}$ are intermediate functions, not meant to be approximations of the solution. Since $\mathscr{M}$ is premultiplied by Δt in (2.19), it may be computed in terms of the intermediate values $U_j^{(0)}$ and $U_j^{(1)}$, without affecting the order of the scheme.

The pseudo-spectral method PS1 possesses a discrete analogue of the conservation law (1.6)

$$\Delta x \sum_j |U_j^{m+1}|^2 = \Delta x \sum_j |U_j^m|^2 = E_0, \tag{2.1.12}$$

but the analogues of (1.7) and (1.8) do not survive the time discretization. The method involves computing the n convolution sums B_k at an $O(n^3)$ cost at each time step.

2.2. *Method PS2*

The $O(n^3)$ cost of forming the B_k terms leads us to reconsider the integration corresponding to the operator $\mathscr{M}_2$, and we use

$$u(x, t_m + \Delta t) = \exp \Delta t \mathscr{M}_2 \cdot u(x, t_m)\colon U^{m+1}$$

$$= \frac{1}{\sqrt{n}} \sum_k \exp -i((2q_m + q_u) |U^m|^2 \mu_k\, \Delta t) \hat{U}_k^m \exp i\mu_k x_j. \tag{2.2.1}$$

If $|U^m|^2$ were constant in space, then (2.2.1) could be efficiently computed by transforming to Fourier space, multiplying each element of the transformed sequence by a constant value and transforming back to physical space. The spatial dependence of $|U^m|^2$, however, compels a convolution in Fourier space, and this is of course the dominant expense associated with method PS1. Here we compute (2.2.1) directly, via a matrix–vector multiplication rather than through the fast Fourier transform.

$$U_j^{(0)} = \exp i(q_c |U_j^m|^2 + q_q |U_j^m|^4)\, \Delta t \cdot U_j^m \tag{2.2.2}$$

$$U_j^{(1)} = \exp -2iq_m \operatorname{Im}(U_j^{(0)} D_x \bar{U}_j^{(0)})\, \Delta t \cdot U_j^{(0)} \tag{2.2.3}$$

$$U_j^{(2)} = \frac{1}{\sqrt{n}} \sum_k \exp -i(2q_m + q_u)\, \mu_k |U_j^{(1)}|^2\, \Delta t \cdot \hat{U}_k^{(1)} \exp i\mu_k x_j \tag{2.2.4}$$

$$U_j^{m+1} = \mathscr{F}_j^{-1}[\exp -i\mu_k^2\, \Delta t \cdot \mathscr{F}_k[U_j^{(2)}]]. \tag{2.2.5}$$

The conservation of mass is no longer guaranteed, but the cost of the method is reduced to $O(n^2)$ operations per time step.

2.3. *Method PS3*

The third split-step method advances according to $\mathscr{L}$ and $\mathscr{N}$ as before, but uses the alternative definition of $\mathscr{M}$, obtained by writing the GNLS as

$$iu_t + u_{xx} + q_c |u|^2 u + q_q |u|^4 u + i(q_m u\bar{u}_x + (q_m + q_u)\bar{u}u_x)u = 0. \tag{2.3.1}$$

This definition of $\mathscr{M}$, explicitly stated as

$$\mathscr{M} = -q_m u\bar{u}_x - (q_m + q_u)\bar{u}u_x, \tag{2.3.2}$$

leads to the integration scheme

$$\begin{aligned} u(x, t_m + \Delta t) &= \exp \Delta t \mathscr{M} \cdot u(x, t_m)\colon U^{m+1} \\ &= \exp -(q_m U^m D_x \bar{U}^m + (q_m + q_u)\bar{U}^m D_x U^m)\, \Delta t \cdot U^m. \end{aligned} \tag{2.3.3}$$

The complete algorithm PS3 comes from applying the split-step method to the semi-discrete system,

$$U_j^{(0)} = \exp i(q_c |U_j^m|^2 + q_q |U_j^m|^4)\, \Delta t \cdot U_j^m \tag{2.3.4}$$

$$U_j^{(1)} = \exp -(q_m U_j^{(0)} D_x \bar{U}_j^{(0)} + (q_u + q_m)\bar{U}_j^{(0)} D_x U_j^{(0)})\, \Delta t \cdot U_j^{(0)} \tag{2.3.5}$$

$$U_j^{m+1} = \mathscr{F}_j^{-1}[\exp -i\mu_k^2\, \Delta t \cdot \mathscr{F}_k[U_j^{(1)}]]. \tag{2.3.6}$$

A straightforward expansion of (2.3.5) reveals that, as with method PS2, the l^2 norm is conserved exactly if $2q_m + q_u = 0$. The computational cost here is further reduced to $O(n \log n)$ operations per time step.

2.4. *Method PS4*

At this point we make the observation that the condition $2q_m + q_u = 0$ obviates the convolution in method PS1, since the step (2.1.10) may then be omitted from the algorithm. The last method we consider is based on solving a new GNLS equation

$$i\psi_t + \psi_{xx} + Q_c |\psi|^2 \psi + Q_q |\psi|^4 \psi + iQ_m |\psi|^2{}_x \psi + iQ_u |\psi|^2 \psi_x = 0. \quad (2.4.1)$$

obtained from (1.1) by the transformation

$$u(x, t) = \psi(x, t) \exp i\theta(x, t), \quad (2.4.2)$$

where the real function θ is defined by

$$\theta_x = -\tfrac{1}{4}(2q_m + q_u) |\psi|^2 \quad (2.4.3)$$

$$\theta_t = -\tfrac{1}{2}(2q_m + q_u) \operatorname{Im}(\psi\bar{\psi}_x). \quad (2.4.4)$$

The new coefficients in (2.4.1) are

$$Q_q = q_q - \tfrac{1}{16}(2q_m + q_u)(2q_m - 3q_u) \quad (2.4.5)$$

$$Q_m = -\tfrac{1}{2}q_u, \quad (2.4.6)$$

with Q_c and Q_u unchanged. We note that the compatibility condition for θ, $\theta_{xt} = \theta_{tx}$, is satisfied by (2.4.1), that $|u| = |\psi|$, and that the transformation works both ways.

The fourth split-step method PS4 is obtained by applying the algorithm as for PS1 to (2.4.1). However, since $2Q_m + Q_u = 0$, the calculation no longer involves the computation of the B_k terms; the step due to $\mathscr{M}_2$ is absent. Since (2.4.1) may be written in the equivalent form

$$i\psi_t + \psi_{xx} + Q_c |\psi|^2 \psi + Q_q |\psi|^4 \psi + Q_u \operatorname{Im}(\psi\bar{\psi}_x)\psi = 0, \quad (2.4.7)$$

the method PS4 reduces to

$$\Psi_j^{(0)} = \exp i(Q_c |\Psi_j^m|^2 + Q_q |\Psi_j^m|^4) \Delta t \cdot \Psi_j^m \quad (2.4.8)$$

$$\Psi_j^{(1)} = \exp iQ_u \operatorname{Im}(\Psi_j^{(0)} D_x \bar{\Psi}_j^{(0)}) \Delta t \cdot \Psi_j^{(0)} \quad (2.4.9)$$

$$\Psi_j^{m+1} = \mathscr{F}_j^{-1}[\exp -i\mu_k{}^2 \Delta t \cdot \mathscr{F}_k[\Psi_j^{(1)}]]. \quad (2.4.10)$$

For the purposes of calculation, we note that the particular choice of $\theta(x, t)$ defined by

$$\theta(x, t) = -\frac{1}{4}(2q_m + q_u)\left(\int_a^x |\psi|^2 \, dx + 2\int_0^t \operatorname{Im}(\psi\bar{\psi}_x) \, dt\Big|_{x=a} + \int^a |\psi(x, 0)|^2 \, dx\right) \quad (2.4.11)$$

satisfies (2.4.3)–(2.4.4) and, following the usual notation with $\Theta_j^m \approx \theta(x_j, t_m)$, can be computed by

$$\Theta_j^m = -\frac{1}{8}(2q_m + q_u)\left(\Delta x \sum_{l=1}^{j} (|\Psi_{l-1}^m| + |\Psi_l^m|^2) + 2\,\Delta t \sum_{p=1}^{m} (\mathrm{Im}(\Psi_{-N/2}^p D_x \bar{\Psi}_{-N/2}^p) + \mathrm{Im}(\Psi_{-N/2}^{p-1} D_x \bar{\Psi}_{-N/2}^{p-1})) \right) + \Theta_{-N/2}^0, \tag{2.4.12}$$

for $m \geqslant 1$. Since $|\psi(x, 0)| = |u(x, 0)|$, Θ_j^0 can be found analytically using the initial condition

$$\Theta_j^0 = -\frac{1}{4}(2q_m + q_u) \int_{x_1}^{x_j} |\psi(x, 0)|^2 \, dx, \tag{2.4.13}$$

and at time t_m, U_j^m is evaluated according to (2.4.2) by

$$U_j^m = \Psi_j^m \exp i\Theta_j^m. \tag{2.4.14}$$

We note that the explicit calculation of U_j^m, and hence of Θ_j^m, at each time step is not necessary to advance Ψ_j^m and consequently, that if only the modulus of the solution is of interest, these computations may be omitted entirely.

This method, by construction, conserves the l^2 norm of the computed solution

$$\Delta x \sum_j |U_j^{m+1}|^2 = \Delta x \sum_j |U_j^m|^2 = E_0. \tag{2.4.15}$$

Being free of the calculation of convolution sums, it requires $O(n \log n)$ operations per time step.

3. Numerical Tests

It is worth mentioning here that the Fourier methods described above are wholly suitable for tracing the evolution of solitary wave solutions of (1.1). The assumption of spatial periodicity is not inappropriate since these solutions are rapidly decreasing functions of x and should therefore be nearly zero at the endpoints of the interval $[a, b]$, provided this interval is not kept unreasonably small.

We compared the four split-step methods on the problems described below; all numerical tests were run on a SUN 3/160 computer.

3.1. *Plane Wave Solution*

The GNLS admits a progressive plane wave solution

$$u(x, t) = A \exp i(\kappa x - \omega t) \tag{3.1.1}$$

with constant amplitude A and nonlinear dispersion relation

$$\omega = \kappa^2 + q_u |A|^2 \kappa - q_c |A|^2 - q_q |A|^4. \tag{3.1.2}$$

All four split-step methods admit identically this nonlinear dispersion relation; that is, if

$$U_j^m = A \exp i(\kappa x_j - \omega t_m) \tag{3.1.3}$$

satisfies the discrete system, then this ω is also defined by Eq. (3.1.2).

For this test, we choose $q_c = q_m = 0$, $q_q = 0.01$, and $q_u = A = \kappa = 1$, so that the theoretical solution is $u(x, t) = \exp i(x - 1.99t)$. We ran the program on the interval $0 \leqslant t \leqslant 3$, with time step $\Delta t = 0.1$. The problem was solved on $-\pi \leqslant x \leqslant \pi$ for methods PS1–PS3 but, to force periodicity on Ψ, on the interval $-\frac{8}{5}\pi \leqslant x \leqslant \frac{8}{5}\pi$ for method PS4.

Methods PS1, PS2, and PS4 produced the correct results, depicted in Fig. 1a (the solution computed by PS4 is truncated to the interval $-\pi \leqslant x \leqslant \pi$). Method PS3 for some time had no difficulty with the problem but, near $t = 3$, suddenly produced erroneous results as shown in Fig. 1b. The problem can be traced to the lack of conservation. The quantities E_0, E_1, and E_2, approximating e_0, e_1, and e_2 respectively, varied only slightly until $t \approx 2.3$, but then the errors grew dramatically as seen in Table I.

When the time step was reduced to $\Delta t = 0.025$, all three quantities remained nearly constant and the method produced the correct results (Fig. 1c). This reduction can only postpone the onset of instabilities related to the nonconservation, however, and the problems observed with the larger time step are likely to appear if the integration is extended over a longer period of time.

TABLE I

Invariants for Plane Wave Solution (Method PS3 with $\Delta t = 0.1$)

t	E_0	E_1	E_2
0.0	6.4795	9.40	−12.566
0.1	6.4795	9.40	−12.566
0.2	6.4795	9.40	−12.566
...	...	...	...
2.1	6.4803	9.47	−12.561
2.2	6.4807	9.62	−12.550
2.3	6.4975	10.14	−12.510
2.4	6.4973	11.87	−12.371
2.5	6.5050	17.80	−11.883
2.6	6.6833	38.34	−10.202
2.7	6.9643	111.17	−4.081
2.8	7.7873	349.40	14.460
2.9	12.8351	1339.73	79.118
3.0	748.9435	79886.07	−1979.741

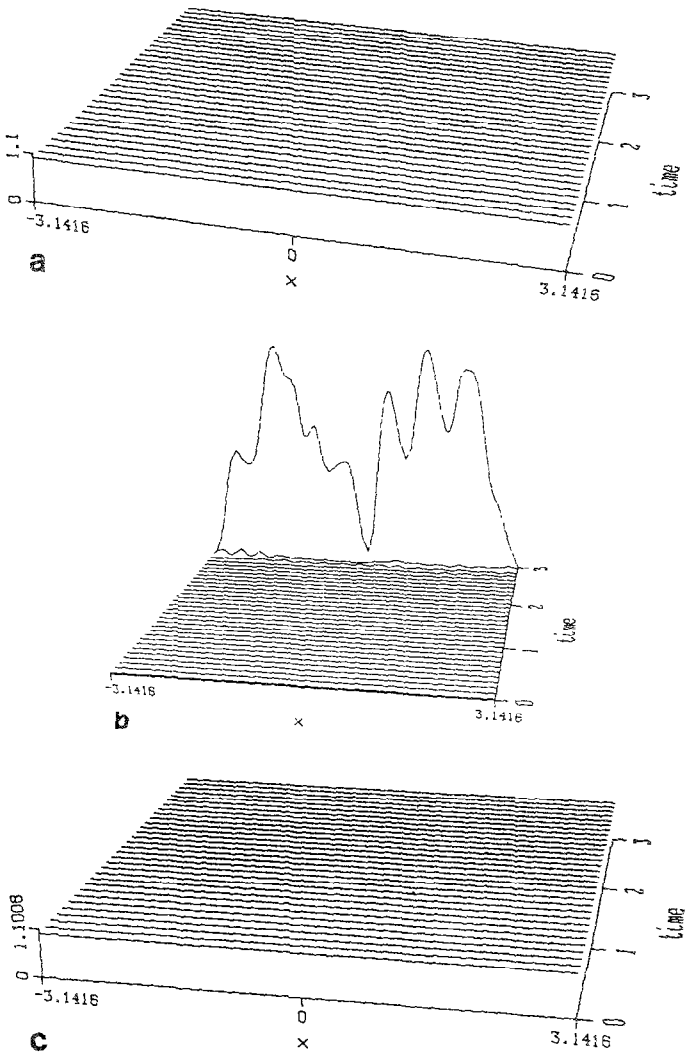

FIG. 1. (a) Plane wave solution (Methods PS1, PS2, PS4) with $\Delta t = 0.1$; (b) Plane wave solution (Method PS3) with $\Delta t = 0.1$; (c) Plane wave solution (Method PS3) with $\Delta t = 0.025$.

The greater E_0 values for method PS4 in Table II are due to solving the transformed GNLS on the larger spatial interval. The results presented in this table also reveal the enormous expense of method PS1. As n increases, the cost of this method becomes prohibitive and so we dismiss it from further consideration.

For this simple test, method PS2 very accurately conserved the l^2 norm and provided an excellent approximation to the solution. This situation does not continue, however, through the more difficult problems considered below.

TABLE II

Comparison of Methods for Plane Wave Solution

Method	n	Δt	l^∞ error	E_0 $(t=0)$	E_0 $(t=3)$	cpu (min)
PS1	32	0.1	2.44990×10^{-4}	6.479535	6.479523	4.402334
PS2	32	0.1	4.88513×10^{-6}	6.479535	6.479533	0.264667
PS3	32	0.025	2.73741×10^{-2}	6.479535	6.479774	0.137000
PS4	32	0.1	1.36836×10^{-4}	10.367256	10.367248	0.037333

3.2. *Solitary Wave Solution*

The GNLS admits a travelling solitary wave solution [12] which, for the choice of coefficients,

$$iu_t + u_{xx} - \tfrac{1}{2}|u|^2 u - \tfrac{7}{4}|u|^4 u - |u|^2{}_x u - 2|u|^2 u_x = 0 \tag{3.2.1}$$

has the form

$$u(x, t) = \left(\frac{4}{4 + 3\sinh^2(x - 2t - 15)}\right)^{1/2} \exp i\phi(x, t) \tag{3.2.2}$$

$$\phi(x, t) = 2\tanh^{-1}(\tfrac{1}{2}\tanh(x - 2t - 15)) + x - 15 \tag{3.2.3}$$

and represents a bell-shaped solitary wave, initially centered at $x = 15$, propagating to the right with speed 2.

For the initial condition $u_0(x)$ corresponding to the above solution, methods PS2, PS3, and PS4 generated the travelling wave depicted in Fig. 2; there were no visible differences in their graphical results. The two notable outcomes of this test were, first, the high computing time required by method PS2 and, second, the higher accuracy of method PS4 (see Table III).

A comment is in order here about the choice of grid parameters Δx and Δt. The finer space discretization required by method PS3 was necessary for reducing the error in the phase (3.2.3). We also found that, although the methods produced the same graphical output using larger time and space steps, a finer resolution was required to obtain acceptable accuracy in the phase of the underlying carrier wave.

TABLE III

Comparison of Methods for Solitary Wave Solution

Method	n	Δt	l^∞ error	E_0 $(t=0)$	E_0 $(t=3)$	cpu (min)
PS2	128	0.001	3.97712×10^{-2}	2.197224	2.169494	372.9927
PS3	256	0.001	1.54745×10^{-2}	2.197224	2.210461	30.14600
PS4	128	0.001	2.90347×10^{-3}	2.197224	2.196960	15.71533

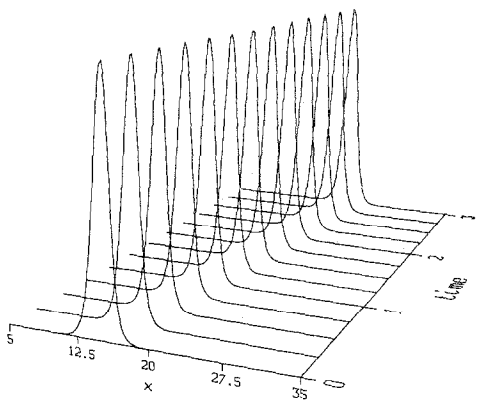

FIG. 2. Solitary wave solution (Methods PS2, PS3, PS4).

It seems that the modulus, or the envelope, of the solution is a more stable quantity than the solution itself; consequently a less stringent discretization would have been sufficient to accurately model the amplitude of the wave.

3.3. *Interacting Solitons*

In this last experiment, we consider interacting solitons for the integrable equation

$$iu_t + u_{xx} + |u|^2 u + |u|^4 u - 2|u|^2{}_x u = 0 \tag{3.3.1}$$

with initial condition

$$u_0(x) = \frac{1}{\sqrt{2}} \operatorname{sech}\left(\frac{1}{2}(x-15)\right) \exp i\left(\frac{1}{2}(x-15) + \tanh\left(\frac{1}{4}(x-15)\right)\right)$$
$$+ \frac{1}{2} \operatorname{sech}\left(\frac{1}{2\sqrt{2}}(x-35)\right) \exp i\left(-\frac{1}{4}(x-35) + \tanh\left(\frac{1}{2\sqrt{2}}(x-35)\right)\right). \tag{3.3.2}$$

The solution consists of two solitary waves, the one initially on the right moving left with unit speed, the one on the left moving right with speed $\frac{1}{2}$. Theoretically, the

TABLE IV

Comparison of Methods for Interacting Solitons

Method	n	Δt	E_0 $(t=0)$	E_0 $(t=20)$	cpu (min)
PS2	128	0.01	2.999657	2.689106	253.9783
PS3	128	0.01	2.999657	3.257465	10.25867
PS4	128	0.01	2.995740	2.995202	4.798667

two solitary waves should emerge from their interaction with their shapes and velocities unchanged, although they may be displaced from the position they would have occupied had the collision not occurred [12].

The problem was solved on the interval $0 \leqslant x \leqslant 50$, up to time $T = 20$. The results are presented in Table IV; for this problem the theoretical L^2 norm of the system is $e_0 = 3$. The disparity in the cpu times of methods PS3 and PS4 should not regarded as typical. In this case, the transformed system (2.4.1) is a cubic NLS in $\psi(x, t)$, and consequently, method PS4 does not evaluate the nonlinear derivative terms (2.4.9).

The solutions computed by the three methods are plotted in Figs. 3a–c. All three methods produced similar results, although we notice some discrepancy during and after the interaction of the solitons. For comparative purposes we include the solution of the cubic Schrödinger equation related to (3.3.1) by the transformation (2.4.2). As expected, these results (Fig. 3d), computed by method PS1, agree exactly with the output of method PS4. The evolution of the theoretically conserved quantities E_0, E_1, and E_2 (Fig. 4) explains the errors of the other two methods. The

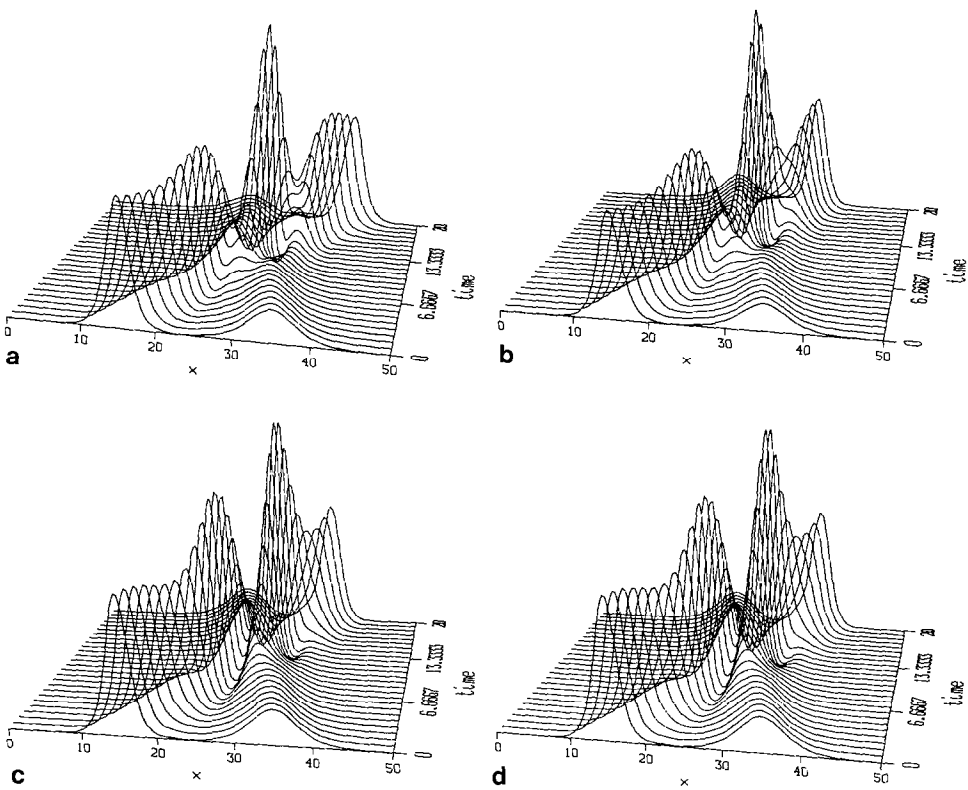

FIG. 3. (a) Interacting solitons (Method PS2); (b) Interacting solitons (Method PS3); (c) Interacting solitons (Method PS4); (d) Interacting solitons for corresponding cubic problem.

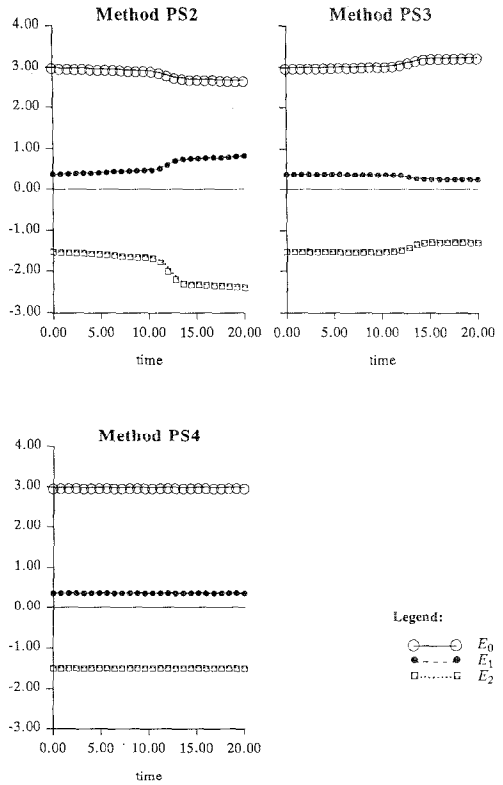

FIG. 4. Conserved quantities (Methods PS2, PS3, PS4) for interacting solitons.

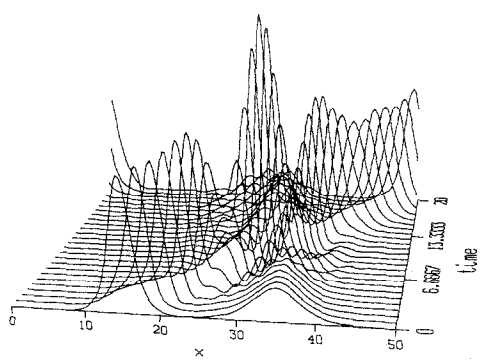

FIG. 5. Interacting solitons (Method PS4) with Θ_j^0 computed by a composite trapezoidal rule.

decrease in the l^2 norm of method PS2 accounts for the discernible flattening of the solitons (Fig. 3a), and its increase as computed by PS3 for the slight steepening (Fig. 3b).

Finally, we note that method PS4 requires an accurate approximation of Θ_j^0; small errors here are magnified and produce substantially incorrect behaviour. Only the initial approximation to $\theta(x, 0)$ has any bearing on the calculation of Ψ_j^m, so that its precise calculation is required just once. When the initial condition $u(x, 0)$ is specified as a continuous function, as it is in all of the tests presented here, then $\theta(x, 0)$ can be found analytically according to (2.4.13). If, on the other hand, the initial condition is specified as discrete data values, then some care must be exercised in evaluating Θ_j^0. In such cases, it is advisable to approximate the integral in Fourier space via a real Fourier transform of $|\Psi_j^0|^2 \equiv |U_j^0|^2$. Figure 5 illustrates the effects of computing Θ_j^0 by a composite trapezoidal approximation of $\int |\psi(x, 0)|^2$. Although the errors in the approximation are typically of the order 10^{-4}, they are progressively magnified and result in changes of speed of the solitons and unclean interactions.

4. Conclusions

We have presented four pseudo-spectral split-step methods for solving a class of nonlinear Schrödinger equations, two of which reflect the mass invariance property of the continuous problem. The advantages of observing this invariance, both in terms of accuracy and stability, are demonstrated through numerical experiments. The mass conservation, when solving the general equation (1.1), exacts a high price through the evaluation of convolution sums. For the class of problems where the coefficients satisfy $2q_m + q_u = 0$, these sums need not be formed for the time integration. The transformation of an arbitrary GNLS to a member of this class therefore provides an efficient means of computing the solution, while observing the l^2 invariance. The precise calculation of the phase difference between the given initial condition and the initial condition in the transformed variable system is necessary, and the solution in the transformed system must be periodic on the spatial domain. For studying solitary wave evolution, this last restriction poses no problem, since the transformed solution will also be a rapidly decreasing function of x.

When solving the GNLS (1.1) directly, the nonconservative method PS3 may be preferable to the conservative scheme, as it dramatically reduces the computing time. The method must be used with some care to ensure that the mass is conserved to within a reasonable tolerance. An adaptive strategy, where the time steps are chosen to avoid large changes in the conserved quantities, would be beneficial here as a safeguard against numerical errors. Alternatively, a conservative method, such as PS1, may be invoked if the nonconservative scheme experiences difficulty in maintaining the invariances.

In conclusion, the behaviour of the quantities E_0, E_1, and E_2 provides a valuable check on the numerical results. In our experience, we found the computed energy

E_1 to be the most sensitive of the three in indicating numerical difficulties and, consequently, the application of any numerical scheme should be accompanied by a close watch on its evolution.

ACKNOWLEDGMENTS

The authors acknowledge the support of the Canadian Natural Sciences and Engineering Research Council made available through a post-graduate scholarship and Grant A3597 The second author was also supported in part by NATO Grant RG0358/82.

REFERENCES

1. R. S. JOHNSON, *Proc. Roy. Soc. London A* **375**, 131 (1977).
2. T. KAKUTANI AND K. MICHIHIRO, *J. Phys. Soc. Japan* **52**, 4129 (1983).
3. F CALOGERO AND W. ECKHAUS, *Inverse Probl.* **3**, 229 (1987).
4. H. HASIMOTO AND H. ONO, *J. Phys. Soc. Japan* **33**, 805 (1972).
5. W. A. STRAUSS, "The Nonlinear Schrödinger Equation," in *Contemporary Developments in Continuum Mechanics*, edited by G. M. de la Penha and L. A. Medeiros (North-Holland, New York, 1978), p. 452.
6. G L. LAMB, JR., *Elements of Soliton Theory* (Wiley, Toronto. 1980).
7. D. KAUP AND A. C. NEWELL, *J. Math. Phys.* **19**, 798 (1978).
8. M. TANAKA, *J. Phys. Soc. Japan* **51**, 2686 (1982).
9. S. COWAN, R. H. ENNS, S. S. RANGNEKAR, AND S. S. SANGHERA, *Canad. J. Phys.* **64**, 311 (1986).
10. A. KUNDU, *Physica D* **25**, 399 (1987).
11. F. CALOGERO AND W. ECKHAUS, *Inverse Probl.* **3**, L27 (1987).
12. D. PATHRIA AND J. LL. MORRIS, Exact solutions for a generalized nonlinear Schrödinger equation, *Phys. Scr.* **39**, 673 (1989).
13. J. M. SANZ-SERNA AND V. S. MANORANJAN, *J. Comput. Phys.* **52**, 273 (1983).
14. M. DELFOUR, M. FORTIN, AND G. PAYRE, *J. Comput. Phys.* **44**, 277 (1981).
15. J. M. SANZ-SERNA AND J. G. VERWER, *IMA J. Numer. Anal.* **6**, 25 (1986).
16. Y. TOURIGNY AND L. LL. MORRIS, *J. Comput. Phys* **76**, 103 (1988).
17. J. W. COOLEY AND J. W. TUKEY, *Math. Comput.* **19**, 297 (1965).
18. E. TADMOR, *SIAM J. Numer. Anal.* **23**, 1 (1986).
19. G. STRANG, *SIAM J. Numer. Anal.* **5**, 506 (1968).
20. R H. HARDIN AND F. D. TAPPERT, *SIAM Rev. Chron.* **15**, 423 (1973).
21. T. R. TAHA AND M. J. ABLOWITZ, *J. Comput. Phys.* **55**, 192 (1984).
22. J. A. C. WEIDEMAN AND B. M. HERBST, *SIAM J. Numer. Anal.* **23**, 485 (1986).
23. A. CLOOT, B. M. HERBST, AND J. A. C. WEIDEMAN, in *Nonlinear Evolutions—Proceedings of the IVth Workshop in Nonlinear Evolution Equations and Dynamical Systems*, edited by J. J.-P. Leon (World Scientific, Singapore, 1987), p. 637.
24. B. M. HERBST, A. R. MITCHELL, AND J. A. C. WEIDEMAN, *J. Comput Phys.* **60**, 263 (1985)